Molecular Crystals and Liquid Crystals Science and Technology. Section A. Molecular Crystals and Liquid Crystals

Publication details, including instructions for authors and subscription information:
http://www.tandfonline.com/loi/gmcl19

Photo- and Electro-Active Amorphous Molecular material: Morphology, Structures, and Hole Transport Properties of Tris[4-(2-Thienyl)Phenyl]Amine

J. I. Sam [a], H. Kageyama [a], S. Nomura [a], H. Nakano [a] & Y. Shirota [a]

[a] Department of Applied Chemistry, Faculty of Engineering, Osaka University, Yamadaoka, Suita, Osaka, 565, Japan

Version of record first published: 24 Sep 2006

To cite this article: J. I. Sam, H. Kageyama, S. Nomura, H. Nakano & Y. Shirota (1997): Photo- and Electro-Active Amorphous Molecular material: Morphology, Structures, and Hole Transport Properties of Tris[4-(2-Thienyl)Phenyl]Amine, Molecular Crystals and Liquid Crystals Science and Technology. Section A. Molecular Crystals and Liquid Crystals, 296:1, 445-463

To link to this article: http://dx.doi.org/10.1080/10587259708032339

Mol. Cryst. Liq. Cryst., 1997, Vol. 296, pp. 445–463
Reprints available directly from the publisher
Photocopying permitted by license only

PHOTO- AND ELECTRO-ACTIVE AMORPHOUS MOLECULAR MATERIAL: MORPHOLOGY, STRUCTURES, AND HOLE TRANSPORT PROPERTIES OF TRIS[4-(2-THIENYL)PHENYL]AMINE

JŪN-ICHI SAKAI, HIROSHI KAGEYAMA, SATOYUKI NOMURA, HIDEYUKI NAKANO, AND YASUHIKO SHIROTA*
Department of Applied Chemistry, Faculty of Engineering, Osaka University, Yamadaoka, Suita, Osaka 565, Japan

Abstract For the purpose of developing photo- and electro-active amorphous molecular materials, tris[4-(2-thienyl)phenyl]amine (TTPA) was synthesized and its molecular and crystal structures, morphological changes, and molecular and hole-transport properties were investigated. TTPA was found to readily form an amorphous glass with a glass-transition temperature of 70 °C, as characterized by differential scanning calorimetry and X-ray diffraction. In addition to the formation of a glass, TTPA was found to exhibit polymorphism. The TTPA glass exhibited a hole drift mobility of 6.4×10^{-4} $cm^2V^{-1}s^{-1}$ at an electric field of 1.0×10^5 Vcm^{-1} at 193 K.

Keywords: amorphous molecular material, tris[4-(2-thienyl)phenyl]amine, glass, polymorphism, molecular and crystal structures, hole drift mobility

INTRODUCTION

Amorphous materials have recently attracted attention as a novel class of functional materials with excellent processability, transparency, isotropic properties, and homogeneous properties owing to the absence of grain boundaries. With regard to amorphous organic materials, polymers and composite polymer systems, where low molecular-weight functional organic materials are dispersed in polymer binders, are known. Although amorphous or quasi-amorphous films of certain organic compounds, *e.g.*, biphenyl, terphenyl, and polycyclic aromatic hydrocarbons such as quaterrylene, naphthacene, and violanthrene can be formed by vacuum deposition at very low

temperatures,[1-8] little attention was paid to low molecular-weight organic compounds that form stable amorphous glasses above room temperature, since low molecular-weight organic compounds generally tend to crystallize readily. Only a few scattered examples of organic compounds that form amorphous glasses above room temperature were known.[9-11]

Low molecular-weight organic compounds that readily form stable glasses with relatively high glass-transition temperatures (Tg) are expected to constitute a novel class of functional organic materials. Creating such amorphous molecular materials is of interest and significance not only from technological applications but also from academic viewpoint, opening up a new field in organic materials science that deals with molecular glasses.

We have designed and synthesized several novel families of organic π-electron systems, which we refer to as "starburst" molecules in view of their molecular structures, for making photo- and electro-active amorphous molecular materials.[12-27] They include 4,4',4"-tris(diphenylamino)triphenylamine and its derivatives[12-14] including 4,4',4"-tri(*N*-carbazolyl)triphenylamine,[15] 4,4',4"-tris(1-naphthylphenylamino)triphenylamine and 4,4',4"-tris(2-naphthylphenylamino)triphenylamine,[16] 1,3,5-tris(diphenylamino)benzene (TDAB) and its derivatives[17-21] including 1,3,5-tris[*N*-(4-diphenylaminophenyl)phenylamino]benzene,[22] 1,3,5-tris[4-(diphenylamino)phenyl]-benzene and its derivatives,[23] tri(biphenyl-4-yl)amine,[24,25] and tri(*p*-terphenyl-4-yl)amine.[24] They are found to readily form amorphous glasses with well-defined glass-transition temperatures except for TDAB. Some of them are found to function as excellent materials for use in organic electroluminescent devices.[15,16,26-28] Recent growing interest in amorphous molecular materials have expanded the scope to include other compounds.[29,30]

The relationship between molecular structure and glass-forming properties is a subject of importance for establishing guidelines for molecular design of amorphous molecular materials. Charge transport in the molecular glass is also a subject of interest. There have been extensive studies on charge transport in molecularly doped polymer systems in view of academic interest and practical application to electrophotography.[31-36] It has recently been revealed that charge transport in molecularly doped polymer systems is greatly affected by the binder polymer.[37-39] It is therefore necessary to investigate charge transport in molecular glasses without a binder polymer in order to elucidate intrinsic charge-transport properties of low molecular-weight organic materials in the disordered system.[23,25,40-43]

We report here on a new amorphous molecular material, tris[4-(2-thienyl)phenyl]-

amine (TTPA). Whereas triphenylamine instantly crystallizes even when the melt sample is rapidly cooled with liquid nitrogen, TTPA is found to readily form an amorphous glass. The morphological changes, molecular and crystal structures, and molecular and hole-transport properties of TTPA are investigated. The results are compared with those of previously reported tri(biphenyl-4-yl)amine.[24,25]

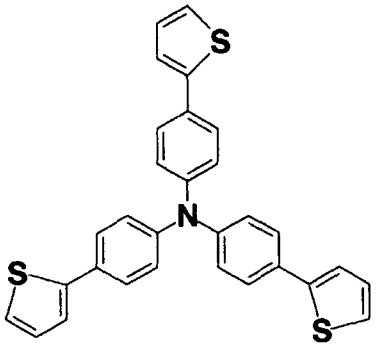

TTPA

EXPERIMENTAL

Materials

Tris(4-iodophenyl)amine was prepared by the reaction of triphenylamine with potassium iodide and potassium iodate in acetic acid at 85 °C for 5 h under nitrogen.[12] 2-Bromothiophene and dichloro[1,3-bis(diphenylphosphino)propane]nickel (II) ($Ni(dppp)Cl_2$) were purchased commercially and used without further purification.

Synthesis of TTPA

A solution of 2-thienylmagnesium bromide, prepared by refluxing a solution of 2-bromothiophene (7.85 g, 48.12 mmol) in 10 ml ether in the presence of magnesium turnings (1.17 g, 48.12 mmol), was added to a solution of tris(4-iodophenyl)amine (5.0 g, 8.02 mmol) in 25 ml THF in the presence of $Ni(dppp)Cl_2$ (42 mg, 0.077 mmol) as a catalyst under nitrogen atmosphere. After the solution was refluxed for 20 h, diluted hydrochloric acid was added to the resulting pale yellow solution at 0 °C to quench the reaction. The solution was extracted with benzene, washed with water, and then dried over sodium sulfate. After removing the solvent, the residue was chromatographed on a silica-gel column using a mixed solvent of benzene and hexane (1:4) as an eluent, followed by recrystallization from hexane to give TTPA as yellow needles (1.35 g, 34.2 %). MS m/z 491 (M^+). Calcd for $C_{30}H_{21}NS_3$: C, 73.61; H, 4.34; N, 2.85%, Found:

C, 73.32; H, 4.28; N, 2.85%. ^{1}H NMR (400 MHz, dioxane-d_8) δ=7.05 (dd, 3H), 7.15 (d, 6H), 7.30 (m, 6H), 7.53 (d, 6H).

Measurements

Cyclic voltammetry was carried out for a dichloromethane solution containing TTPA (1.0×10^{-3} mol dm^{-3}) and tetrabutylammonium perchlorate (0.1 mol dm^{-3}), by using platinum plates as the working and counter electrodes and $Ag/AgNO_3$ (0.01 mol dm^{-3} in acetonitrile) as the reference electrode.

Morphological changes were examined by differential scanning calorimetry (DSC) and X-ray diffraction.

Hole drift mobility was measured by a time-of-flight method using a layered device which consists of a charge-carrier generation layer (CGL) and a charge-carrier transport layer (CTL). An appropriate amount of TTPA was melted on an ITO glass to form a film of 10 ~ 20 μm thickness, and pressed onto another ITO glass on which X-type metal free phthalocyanine dispersed in poly(ethylene-co-vinylchloride) as CGL was coated by a spin-coat method. A polyimide spacer was used to achieve a uniform thickness. The thickness of the sample was measured with a micrometer. The cell was mounted in a cryostat and irradiated with pulsed white light through a UV-37 glass filter (Toshiba Corp.) from a xenon stroboscopic lamp (pulse duration time : 1 ~ 4 μs). The temperature of the sample was controlled by a temperature controller, ITC 502 (Oxford). Hole carriers photogenerated in the CGL are injected into the CTL at time zero and transported across the TTPA layer under an external electric field. The photocurrent was converted to the voltage using an amplifier, LI-76 (NF Circuit), and monitored using a digital storage scope, KDS-102 (Kawasaki Electronica).

X-Ray Crystal Structure Analysis of TTPA

Since a good quality single crystal of TTPA for X-ray crystal structure analysis could not be obtained by recrystallization from hexane, a single crystal was grown from a benzene solution to give a prism with dimensions of approximately 0.15 x 0.23 x 0.38 mm^3, which contains the solvent molecule benzene. The crystal data were as follows: $C_{30}H_{21}NS_3(C_6H_6)_{0.5}$, M=530.74, monoclinic, space group $P2_1/c$, a=13.311(4), b=17.869(5), c=11.662(5) Å, β=101.71(3)°, V=2716(2) Å^3, Z=4, Dc=1.30 gcm^{-1}, μ(Mo Kα)=3.01 cm^{-1}.

X-Ray diffraction data were collected by the ω-2θ scan technique up to 2θ=55° on Rigaku AFC-5R automatic four-circle diffractometer using graphite monochromatized Mo Kα radiation (λ=0.7107 Å). No significant intensity decay of three standard reflections was detected as measured after every 150 reflections. Of the 6752

reflections measured, 1946 reflections were observed ($|F_o| > 3\sigma(F_o)$). The intensity data were corrected for the Lorentz and polarization effects, but not for absorption.

The structure was solved by a direct method (SAPI91)[44] and expanded using Fourier technique (DIRDIF).[45] The structure was refined anisotropically for all the non-hydrogen atoms by a full-matrix least-squares method. During the refinement process, two thienyl groups (T2 and T3) of the TTPA molecule were found to be disordered; each takes two positions differing about 180° around the C-C single bond connecting the thienyl group and the phenyl group. Thus, the structure refinement was carried out under the following conditions. (i) The positional parameters and temperature factors of C20, C23, C31, and C34 were assumed to be equal to those of S20, S23, S31, and S34, respectively. (ii) The site occupancy factors (sof) of S20, S23, S31, S34, C20, C23, C31, and C34 were refined under the following conditions;

$$\text{sof(S20)} = 1 - \text{sof(S23)} = 1 - \text{sof(C20)} = \text{sof(C23)}$$
$$\text{sof(S31)} = 1 - \text{sof(S34)} = 1 - \text{sof(C31)} = \text{sof(C34)}$$

(iii) The hydrogen atoms in the disordered thienyl groups and the solvent benzene molecule were omitted from the calculation and the other hydrogen atoms were located at their calculated positions. Their isotropic temperature factors were assumed to be equal to the equivalent temperature factors of the carbon atoms bonded.

The function minimized was $\Sigma w(|F_o|-|F_c|)^2$, where the weighting function was $w=1/\sigma^2(F_o)$. The atomic scattering factors were taken from those of the International Tables for X-Ray Crystallography.[46] The R and Rw values at the last stage were 0.088 and 0.059, respectively. All calculations were performed using the TEXSAN crystallographic software package of Molecular Structure Computation[47] by a workstation (INDIGO R4000, Silicon Graphics) at the Department of Applied Chemistry, Faculty of Engineering, Osaka University. The atomic coordinates of the non-hydrogen atoms with the equivalent temperature factors[48] are given in Table 1.

Apparatus

Electronic absorption and fluorescence spectra were taken on a Hitachi U-3200 spectrophotometer and a Hitachi 850 fluorescence spectrophotometer, respectively. DSC measurement was made using a Seiko DSC220C. X-Ray diffraction measurement was carried out with a M18XHF-SRA X-ray diffractometer (MAC Science). Cyclic voltammetry was carried out with a Hokuto Denko HA-501 Potentiostat and a HB-104 Function Generator. For the measurement of hole drift mobilities, voltage was applied to the layered device using a Takasago TMD0360-022 regulated DC power supply.

TABLE I Positional parameters, equivalent temperature factors, and site occupancy factors (sof) for non-hydrogen atoms of TTPA$(C_6H_6)_{0.6}$.

atom	x	y	z	B(eq)	sof
S(9)	-0.4938(3)	-0.6885(2)	-0.6278(3)	9.3(1)	
S(20)	-0.0482(3)	-0.7443(3)	0.2791(4)	6.6(2)	0.585
S(23)	-0.0180(4)	-0.6127(4)	0.3879(6)	8.2(2)	0.415
S(31)	-0.2960(6)	-0.1350(4)	-0.0665(7)	7.1(3)	0.251
S(34)	-0.2076(3)	-0.1264(2)	-0.2464(3)	5.5(1)	0.749
N(1)	-0.2325(7)	-0.4996(5)	-0.1593(8)	5.3(3)	
C(2)	-0.266(1)	-0.5402(6)	-0.2666(9)	4.3(3)	
C(3)	-0.3685(9)	-0.5355(6)	-0.324(1)	4.9(3)	
C(4)	-0.4025(8)	-0.5767(6)	-0.424(1)	4.6(3)	
C(5)	-0.3346(8)	-0.6212(6)	-0.4695(8)	3.5(3)	
C(6)	-0.2327(8)	-0.6239(6)	-0.411(1)	4.2(3)	
C(7)	-0.1981(8)	-0.5837(6)	-0.310(1)	4.7(3)	
C(8)	-0.3695(7)	-0.6655(6)	-0.5772(9)	3.9(3)	
C(10)	-0.466(1)	-0.7390(8)	-0.742(1)	7.8(4)	
C(11)	-0.368(1)	-0.7377(8)	-0.742(1)	6.9(4)	
C(12)	-0.3099(8)	-0.6948(6)	-0.650(1)	5.1(3)	
C(13)	-0.1894(9)	-0.5377(7)	-0.057(1)	4.5(3)	
C(14)	-0.2147(8)	-0.6109(7)	-0.036(1)	5.1(3)	
C(15)	-0.1712(9)	-0.6480(6)	0.067(1)	5.1(4)	
C(16)	-0.0998(8)	-0.6138(7)	0.157(1)	4.8(4)	
C(17)	-0.0739(8)	-0.5413(7)	0.135(1)	5.2(3)	
C(18)	-0.1165(9)	-0.5038(6)	0.033(1)	5.0(3)	
C(19)	-0.0574(7)	-0.6544(8)	0.268(1)	5.4(4)	
C(20)	-0.0482	-0.7443	0.2791	6.6	0.415
C(21)	0.000(1)	-0.750(1)	0.417(2)	9.4(6)	
C(22)	0.015(1)	-0.681(1)	0.468(1)	9.0(5)	
C(23)	-0.0180	-0.6127	0.3879	8.2	0.585
C(24)	-0.2404(9)	-0.4219(6)	-0.159(1)	4.5(3)	
C(25)	-0.2798(9)	-0.3836(7)	-0.074(1)	5.1(4)	
C(26)	-0.2851(8)	-0.3055(6)	-0.0749(9)	4.6(3)	
C(27)	-0.2537(7)	-0.2612(6)	-0.1590(9)	3.8(3)	
C(28)	-0.2182(8)	-0.3029(6)	-0.2470(9)	4.8(3)	
C(29)	-0.2132(9)	-0.3802(7)	-0.247(1)	5.1(3)	
C(30)	-0.2567(7)	-0.1805(5)	-0.153(1)	3.9(3)	
C(31)	-0.2960	-0.1350	-0.0665	7.1	0.749
C(32)	-0.279(1)	-0.0552(7)	-0.093(1)	7.7(5)	
C(33)	-0.233(1)	-0.0448(6)	-0.187(1)	6.4(4)	
C(34)	-0.2076	-0.1264	-0.2464	5.5	0.251
C(35)	-0.475(2)	-0.043(2)	-0.397(3)	10.6(9)	
C(36)	-0.529(2)	-0.077(1)	-0.501(5)	10.7(7)	
C(37)	-0.554(2)	-0.032(3)	-0.603(2)	10.5(8)	

The photocurrent was monitored using a Kawasaki Electronica KDS-102 digital storage scope.

RESULTS

Molecular Properties

TTPA shows an electronic absorption band with λ_{max} at 363 nm (log ε = 4.8) and a fluorescence band with λ_{max} at 422 nm. The fluorescence quantum yield of TTPA in a THF solution was determined to be 0.68.

TTPA shows a reversible anodic oxidation process, as characterized by cyclic voltammetry. The half-wave oxidation potential of TTPA ($E^{ox}_{1/2}$) in dichloromethane was determined to be 0.57 V *vs.* Ag/Ag^+ (0.01 mol dm^{-3}). The second oxidation process of TTPA was irreversible.

Glass Formation and Polymorphism

It was found that TTPA readily forms an amorphous glass when the melt sample was cooled either rapidly with liquid nitrogen or slowly on standing in air. In addition to the formation of a glass, TTPA was found to exhibit polymorphism. Figure 1 shows DSC curves of TTPA. When a crystalline sample of TTPA (crystal A) obtained by recrystallization from hexane was heated, an endothermic peak due to melting was observed at 185 °C. When the melt sample was cooled down either rapidly with liquid nitrogen or slowly on standing in air, it formed an amorphous glass *via* a supercooled liquid state. When the glass sample was heated, glass transition took place at 70 °C. On heating above the Tg, crystallization occurred at 119 °C to form another crystal (crystal B). On further heating, an exothermic peak due to solid-solid phase transformation from the crystal B to the crystal A was observed at 134 °C, followed by the melting of the crystal A at 185 °C. The same trace was observed over many cycles.

The formation of the glass and the crystals A and B was evidenced by X-ray diffraction (Figure 2). The crystalline sample formed by heating the glass to *ca.* 160 °C exhibits the same sharp diffraction peaks as those of the crystal A obtained by recrystallization from hexane. The crystalline sample formed by heating the glass to *ca.* 130 °C exhibits new peaks which are not observed for the crystal A. This indicates the formation of a different crystal form (crystal B) at this temperature, which undergoes the solid-solid phase transformation from the crystal B to the crystal A on heating, as evidenced from the DSC curve. On the other hand, the glass obtained by cooling the melt sample exhibited only a broad halo. The morphological changes of TTPA are summarized in Scheme 1.

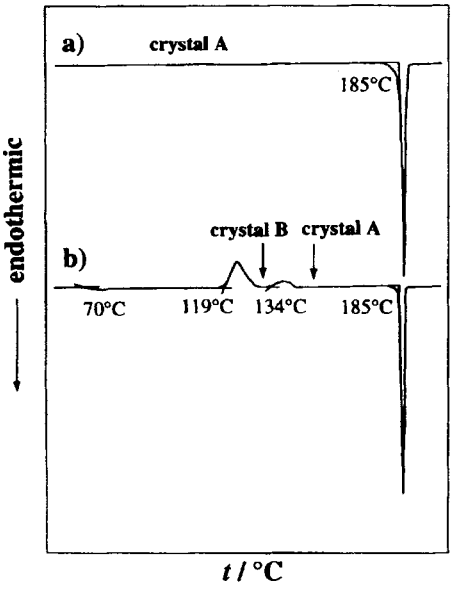

FIGURE 1 DSC curves of TTPA.
a) Recrystallized sample (crystal A) was heated. b) Amorphous glass obtained by cooling the melt was heated.
Heating rate: 1 °Cmin^{-1}.

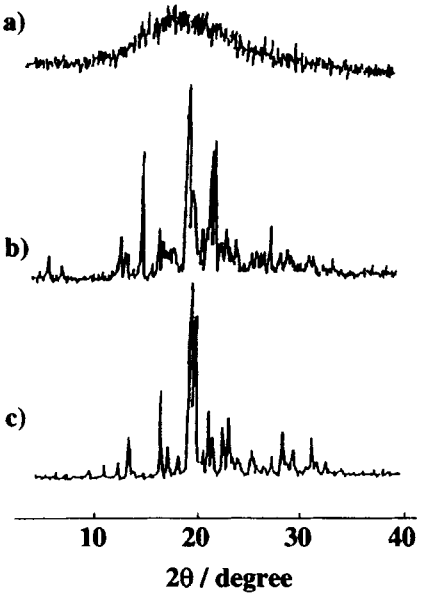

FIGURE 2 X-Ray diffraction patterns of TTPA for a) the glass sample obtained by cooling the melt, and the crystalline samples obtained by heating the glass to b) *ca.* 130 °C and c) *ca.* 160 °C.

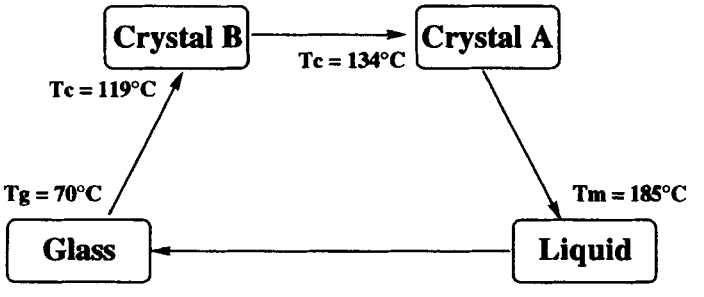

SCHEME 1 Morphological changes of TTPA.

Molecular and Crystal Structures

Determination of molecular and crystal structures is expected to provide information on the relationship between molecular structure and glass-forming properties. The TTPA crystal submitted to X-ray crystal structure analysis was grown from a benzene solution, which contained the solvent molecule benzene in a molar ratio of TTPA:C_6H_6 = 2:1. The atomic coordinates of non-hydrogen atoms with equivalent temperature factors and site occupancy factors (sof) are listed in Table I.

Figure 3 shows the molecular structure of TTPA in the crystal of TTPA$(C_6H_6)_{0.5}$, where the three phenyl and thienyl rings in TTPA are referred to as P1, P2, and P3, and T1, T2, and T3, respectively. The central triphenylamine moiety has a propeller-like structure. That is, the dihedral angles between the plane consisting of the three carbon atoms bonded to the nitrogen atom and the least square planes of the phenyl rings P1, P2, and P3 are 59.7, 27.8, and 45.9°, respectively. The nitrogen atom deviates from the plane consisting of the three carbon atoms bonded to the nitrogen atom and the distance between the plane and the nitrogen atom is 0.01 Å. In addition, the thienyl groups are twisted against the phenyl groups bonded. When viewed from the nitrogen atom in Figure 3, the thienyl ring T2 is twisted clockwise by 26.4° against the inside phenyl ring P2, while the thienyl rings T1 and T3 are twisted counterclockwise by 20.2 and 6.5°,

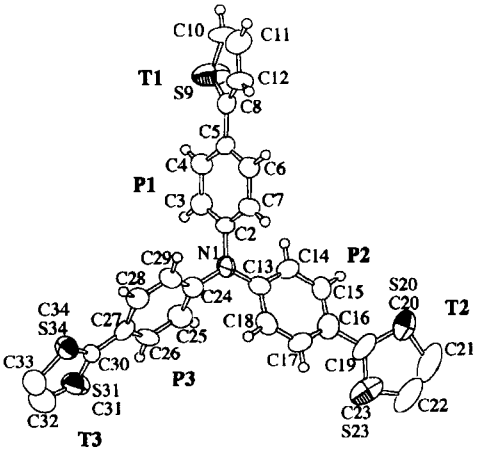

FIGURE 3 Molecular structure of TTPA.

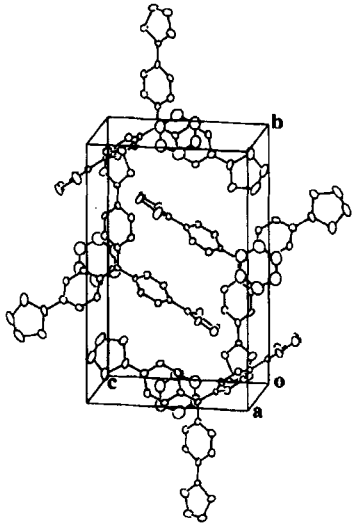

FIGURE 4 Crystal structure of TTPA$(C_6H_6)_{0.5}$.

respectively, against the corresponding inside phenyl rings P1 and P3. The two thienyl groups, T2 and T3, were found to be disordered; each takes two positions differing about 180° around the C-C single bond connecting the thienyl group and the phenyl group. The population ratios of the disordered thienyl groups T2 and T3 were estimated from the values of site occupancy factors (sof) of sulfur atoms; sof(S20):sof(S23) and sof(S20):sof(S34) were 0.59:0.41 and 0.25:0.75, respectively.

Figure 4 shows the crystal structure of TTPA$(C_6H_6)_{0.5}$. There are four TTPA and two benzene molecules in a unit cell without any significant short intermolecular contact.

Charge Transport in the Glassy State

The transient photocurrent observed for the TTPA glass was nearly nondispersive, as shown in Figure 5. The transit time (τ_t) was determined from the plot of log i_{ph} *vs.* log t, where i_{ph} and t represent transient photocurrent and time, respectively, according to the Scher-Montroll theory.[49] The hole drift mobility was calculated from the transit time (τ_t) from the equation $\mu = L^2/\tau_t V$, where L is the thickness of CTL and V the applied voltage.

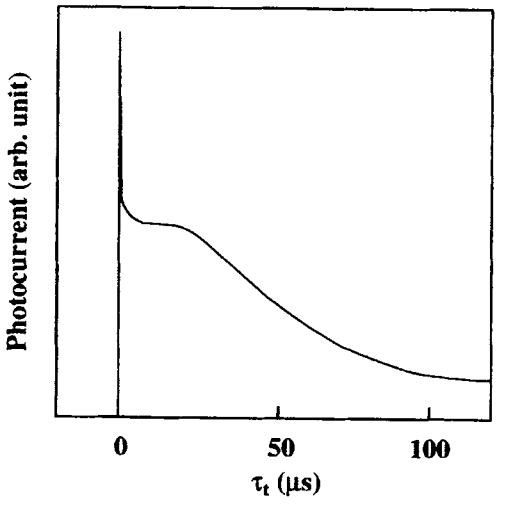

FIGURE 5 Typical transient photocurrent observed for a TTPA glass.

The hole drift mobility of TTPA in the glassy state was measured in the temperature range from 108 K to 193K. The hole drift mobility of TTPA in the glassy

state at an electric field of 1.0 x 10^5 Vcm^{-1} was determined to be 3.1 x 10^{-6} and 6.4 x 10^{-4} $cm^2V^{-1}s^{-1}$ at 108 K and 193 K, respectively.

The electric-field and temperature dependencies of the hole drift mobility of the TTPA glass were analyzed in terms of both the empirical equation[31] and the disorder formalism.[35,36]

The empirical equation, which takes the Poole-Frenkel model into account, is described as equation 1;

$$\mu = \mu_0 \exp\left(-\frac{E_0 - \beta_{PF}E^{1/2}}{kT_{eff}}\right) \qquad (1)$$
$$T_{eff}^{-1} = T^{-1} - T_0^{-1}$$

where E_0 is the activation energy at the zero electric field, β_{PF} the Poole-Frenkel coefficient, k_B the Boltzmann's constant, E the electric field, and T_0 the temperature at which the extrapolated data of Arrhenius plots at various electric fields intersect with one another, and μ_0 the mobility at T_0.

The disorder formalism, which assumes that charge transport occurs by hopping through a manifold of localized states with superimposed positional disorder, is described by equation 2;

$$\mu(\hat{\sigma},\Sigma,E) = \mu_0 \exp\left[-\left(\frac{2}{3}\hat{\sigma}\right)^2\right]\exp\left[C\left(\hat{\sigma}^2 - \Sigma^2\right)E^{1/2}\right] \qquad (2)$$
$$\hat{\sigma} = \frac{\sigma}{kT}$$

where σ is the width of the Gaussian density of states, Σ a parameter that characterizes the degree of positional disorder, μ_0 a hypothetical mobility in the disorder-free system, E the electric field, and C an empirical constant.

Figure 6 shows that the electric-field dependence of the hole drift mobility in the TTPA glass follows $\exp(\beta E^{1/2})$.

The temperature dependence of the hole drift mobility was found to be fit to both Eq. 1 and Eq. 2. Figure 7 shows Arrhenius plots of the hole drift mobility of the TTPA glass at several electric fields. The apparent activation energy (E_{act}) for charge transport at each electric field was obtained from the slope of the linear plots. The activation energy at the zero electric field (E_0) was determined by extrapolating the plot of E_{act} *vs.* $E^{1/2}$ to the zero electric field, as shown in Figure 8.

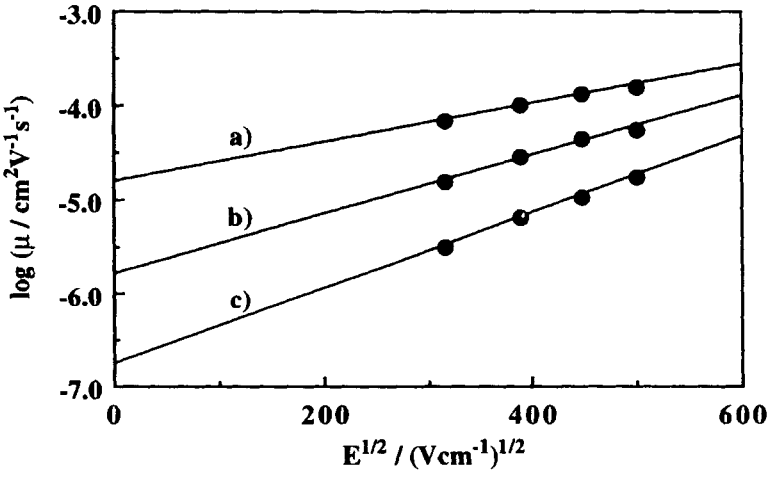

FIGURE 6 Electric-field dependencies of the hole drift mobility of the TTPA glass at different temperatures: a) 148 K, b) 128 K, and c) 108 K.

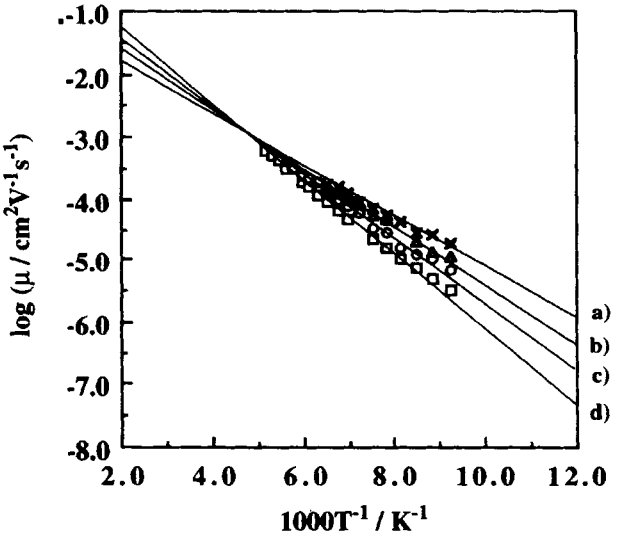

FIGURE 7 Arrhenius plots of the hole drift mobility of the TTPA glass at different electric fields: a) 2.5 x 10^5, b) 2.0 x 10^5, c) 1.5 x 10^5, d) 1.0 x 10^5 Vcm^{-1}.

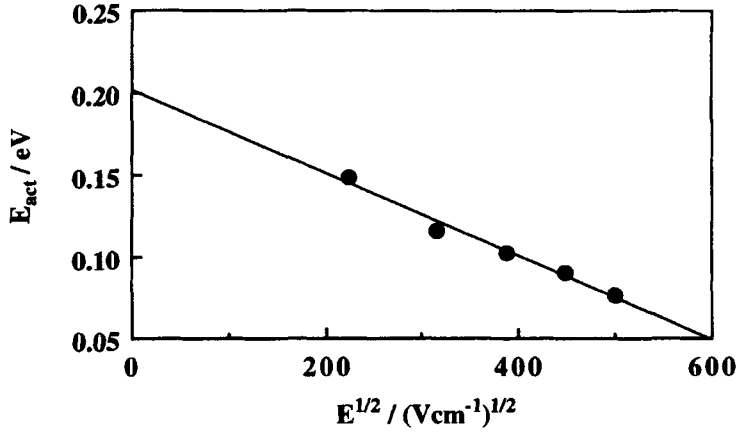

FIGURE 8 Plots of activation energies (E_{act}) *vs.* $E^{1/2}$.

Figure 9 shows the plots of log $\mu(E=0)$ *vs.* T^{-2} for the TTPA glass, where $\mu(E=0)$ is the hole drift mobility at the zero electric field determined by extrapolating the plots of log μ *vs.* $E^{1/2}$ to the zero electric field. The parameters σ and μ_0 were obtained from the slope and the intercept, respectively, of the linear plots extrapolated to $T\rightarrow\infty$. Eq. 2 predicts that the slope of the electric-field dependence of hole drift mobilities ($S=\partial\ln(\mu/\mu_0)/\partial E^{1/2}$) should be linearly dependent upon $\hat{\sigma}^2$ with a slope of C. Figure 10 shows the plots of S *vs.* $\hat{\sigma}^2$. As predicted, a linear relationship was observed, and

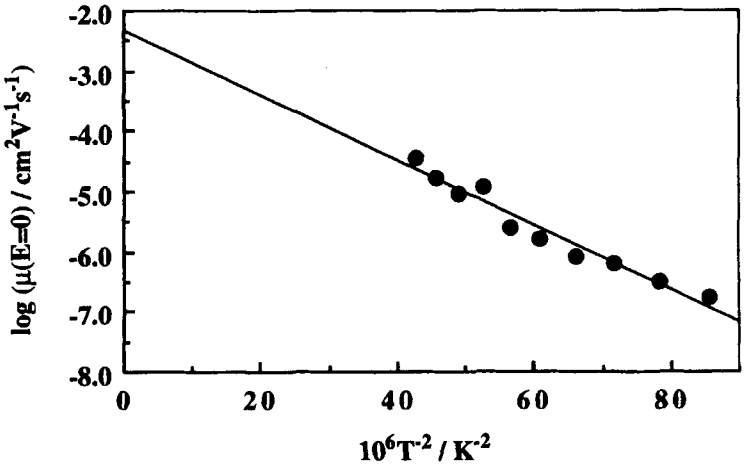

FIGURE 9 Plots of the logarithm of hole drift mobilities at the zero electric field *vs.* T^{-2}.

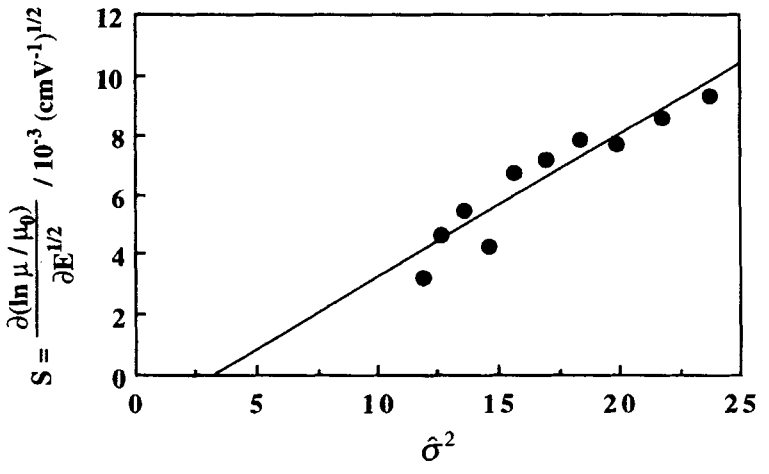

FIGURE 10 Plots of S vs. $\hat{\sigma}^2$.

the value Σ was determined from the intersection of the linear plots at S=0, where $\hat{\sigma}^2=\Sigma^2$ holds.

The charge transport parameters in Eq. 1, μ_0, E_0, T_0, and β_{PF}, and those in Eq. 2, μ_0, σ, Σ, and C, for TTPA are summarized in Table II.

TABLE II Hole-transport parameters for the TTPA glass based on Eq. 1 and Eq. 2.

Based on Eq.1			
$\mu_0 = 1.0 \times 10^{-3}$ cm^{2}V^{-1}s^{-1}	$E_0 = 0.20$ eV	$T_0 = 213$ K	$\beta_{PF} = 2.6 \times 10^{-4}$ eV(cmV^{-1})$^{1/2}$
Based on Eq.2			
$\mu_0 = 4.5 \times 10^{-3}$ cm^{2}V^{-1}s^{-1}	$\sigma = 0.05$ eV	$\Sigma = 1.7$	$C = 3.0 \times 10^{-4}$ (cmV^{-1})$^{1/2}$

DISCUSSION

In the present study, TTPA was found to form an amorphous glass with a well-defined, relatively high Tg of 70 °C. The results of X-ray crystal structure analysis for a TTPA crystal show that TTPA has a nonplanar structure. It is thought that the nonplanar molecular structure plays an important role in the formation of a glass. That is, the nonplanar molecular structure prevents the ready packing of molecules to form a crystal. In addition, the existence of different conformers is suggested to facilitate the formation of the glass as discussed below.

As compared with tri(biphenyl-4-yl)amine,[25] TTPA forms an amorphous glass

more readily. That is, whereas tri(biphenyl-4-yl)amine requires rapid cooling of the melt sample at a cooling rate faster than *ca.* 30 °C min^{-1} to form an amorphous glass, TTPA forms a glass even when the melt sample is cooled at a cooling rate as slow as 1 °C min^{-1}. This result shows that the replacement of the phenyl groups in tri(biphenyl-4-yl)amine by the three thienyl groups makes glass formation easier. We have previously reported that whereas 1,3,5-tris(diphenylamino)benzene (TDAB) readily crystallizes even when the melt is rapidly cooled with liquid nitrogen, 1,3,5-tris(phenyl-2-thienylamino)benzene (α-TPTAB) and 1,3,5-tris(phenyl-3-thienylamino)benzene (β-TPTAB), where the three phenyl groups in TDAB are replaced by the thienyl group, form amorphous glasses.[20] It is suggested that the replacement of the three phenyl groups in tri(biphenyl-4-yl)amine and TDAB by three asymmetric aromatic thienyl groups increases the number of conformers of the molecules, facilitating glass formation. The increase in the number of conformers is supported by the result of the X-ray crystal structure analysis that the TTPA, α-TPTAB, and β-TPTAB molecules have disordered structures due to the thienyl group. Such disordered structures have also been reported for other compounds containing the thienyl group.[50-52]

It is shown that the TTPA glass, which is in the thermodynamically nonequilibrium state, is transformed into a thermodynamically equilibrium, metastable supercooled liquid at Tg, finally producing the crystal A *via* the metastable crystal B, as illustrated by the schematic free energy - temperature curves (Figure 11). This phenomenon of polymorphism observed for TTPA suggests that different conformers exist for TTPA. The existence of different conformers is thought to prevent the packing of the molecules, facilitating glass formation.

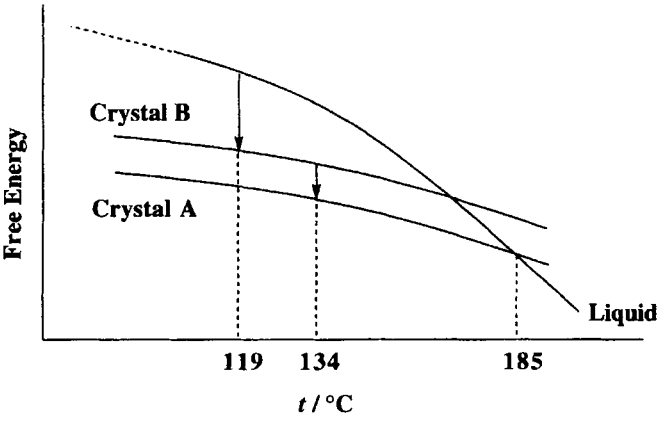

FIGURE 11 Schematic free energy - temperature curves for TTPA.

It was found that the TTPA glass exhibits a hole drift mobility of 6.4 x 10^{-4} $cm^2V^{-1}s^{-1}$ at an electric field of 1.0 x 10^5 Vcm^{-1} at 193 K. This is a high value among organic disordered systems. We have shown that the glasses of tri(biphenyl-4-yl)amine and 4-diphenylaminobenzaldehyde diphenylhydrazone (DPH) exhibit hole drift mobilities of 2.9 x 10^{-6} and 3.1 x 10^{-6} $cm^2V^{-1}s^{-1}$, respectively, under the same conditions. The hole drift mobilities in molecularly doped polymer systems are 4.6 x 10^{-8} $cm^2V^{-1}s^{-1}$ for 50 wt% DPH-doped polycarbonate system at 1.0 x 10^5 Vcm^{-1} at 200 K and 2 x 10^{-8} $cm^2V^{-1}s^{-1}$ for the 40 wt% tri(*p*-tolyl)amine-doped polycarbonate system at an electric field of 9 x 10^4 Vcm^{-1} at 218 K.[53] The higher mobilities of molecular glasses than those of molecularly doped polymer systems are thought to be due to shorter intersite distances and less fluctuations of hopping site energies. The hole drift mobility of TTPA is found to be higher than those for other molecular glasses. It is thought that the smaller values of E_0 in terms of Eq. 1 and σ in terms of Eq. 2 are partly responsible for higher charge-carrier mobility of the TTPA glass, and that the molecular structure plays an important role in the hole transport properties of molecular glasses. Further studies are in progress to investigate charge transport in a wider temperature range.

SUMMARY

It is found that TTPA readily forms an amorphous glass with a relatively high Tg of 70 °C, constituting a new photo- and electro-active amorphous molecular material and that the TTPA glass exhibits a high hole drift mobility approaching to 10^{-3} $cm^2V^{-1}s^{-1}$. It is expected that TTPA functions as a good charge transport material for use in photoreceptors in electrophotography and for use in organic electroluminescent devices.

DEDICATION

This paper is dedicated to Professors Yusei Maruyama and Fumio Ogura on the occasion of their retirement from Institute for Molecular Science and Hiroshima University, respectively, for their outstanding achievements in the research fields of solid state science and materials chemistry.

REFERENCES

1. E. A. Silinsh, Organic Molecular Crystals, (Springer-Verlag, Berlin, 1980).

2. R. J. Green and D. Turnbull, J. Phys. Chem. 46, 1243 (1967).
3. Y. Maruyama, T. Iwaki, T. Kajiwara, I. Shirotani, and H. Inokuchi, Bull. Chem. Soc. Jpn. 43, 1259 (1970).
4. Y. Maruyama and N. Iwasaki, Chem. Phys. Lett. 24, 26 (1974).
5. Y. Maruyama and T. Yamada, J. Non-Cryst. Solids 28, 143 (1978).
6. T. Onaka-Ito, and Y. Maruyama, Mol. Cryst. Liq. Cryst. 91, 187 (1983).
7. H. Nakayama, M. Kawahara, K. Tanabe, K. Ishii, Mol. Cryst. Liq. Cryst. 218, 183 (1992).
8. K. Ishii, H. Nakayama, K. Tanabe, and M. Kawahara, Chem. Phys. Lett. 198, 236 (1992).
9. B. Rosenberg, J. Chem. Phys. 31, 238 (1959).
10. D. J. Plazek and J. H. Magill, J. Chem. Phys. 45, 3038 (1966).
11. Y. Sano, K. Kato, M. Yokoyama, Y. Shirota, and H. Mikawa, Mol. Cryst. Liq. Cryst. 36, 137 (1976).
12. Y. Shirota, T. Kobata, and N. Noma, Chem. Lett., 1145 (1989).
13. A. Higuchi, H. Inada, and Y. Shirota, Adv. Mater. 3, 549 (1991).
14. A. Higuchi and Y. Shirota, Mol. Cryst. Liq. Cryst. 242, 127 (1994).
15. Y. Kuwabara, H. Ogawa, H. Inada, N. Noma, and Y. Shirota, Adv. Mater. 6, 677 (1994).
16. D. Okuda, H. Inada and Y. Shirota, Ann. Meeting of Jpn. Chem. Soc., Preprint, 635 (1995); submitted for publication in J. Luminescence.
17. W. Ishikawa, H. Inada, H. Nakano and Y. Shirota, Chem. Lett., 1731 (1991).
18. W. Ishikawa, H. Inada, H. Nakano and Y. Shirota, Mol. Cryst. Liq. Cryst. 211, 431 (1992).
19. W. Ishikawa, H. Inada, H. Nakano, and Y. Shirota, J. Phys. D : Appl. Phys. 26, B94 (1993).
20. E. Ueta, H. Nakano, and Y. Shirota, Chem. Lett., 2397 (1994).
21. H. Kageyama, K. Itano, W. Ishikawa, and Y. Shirota, J. Mater. Chem. 6, 675 (1996).
22. W. Ishikawa, K. Noguchi, Y. Kuwabara, and Y. Shirota, Adv. Mater. 5, 559 (1993).
23. H. Inada and Y. Shirota, J. Mater. Chem. 3, 319 (1993).
24. A. Higuchi, K. Ohnishi, S. Nomura, H. Inada, and Y. Shirota, J. Mater. Chem. 2, 1109 (1992).
25. H. Inada, K. Ohnishi, S. Nomura, A. Higuchi, H. Nakano, and Y. Shirota, J. Mater. Chem. 4, 171 (1994).

26. Y. Shirota, Y. Kuwabara, H. Inada, T. Wakimoto, H. Nakada, Y. Yonemoto, S. Kawami, and K. Imai, Appl. Phys. Lett. 65, 807 (1994).
27. H. Inada, Y. Yonemoto, T. Wakimoto, K. Imai, and Y. Shirota, Mol. Cryst. Liq. Cryst. 280, 331 (1996).
28. Y. Hamada, T. Sano, K. Shibata, and K. Kuroki, Jpn. J. Appl. Phys. 34, L824 (1995).
29. K. Naito and A. Miura, J. Phys. Chem. 97, 6240 (1993).
30. Y. H. Kim and R. Beckerbauer, Macromolecules 27, 1968 (1994).
31. W. D. Gill, J. Appl. Phys. 43, 5033 (1972).
32. M. Stolka, J. F. Yanus and D. M. Pai, J. Phys. Chem. 88, 4707 (1984).
33. J. X. Mack, L. B. Schein and A. Peled, Phys. Rev. B 39, 7500 (1989).
34. L. B. Schein, D. Glatz and J. C. Scott, Phys. Rev. Lett. 65, 472 (1990).
35. H. Bässler, Phys. Status Solidi B 107, 9 (1982).
36. H. Bässler, Phys. Status Solidi B 175, 15 (1993).
37. T. Sasakawa, T. Ikeda and S. Tazuke, J. Appl. Phys. 65, 2750 (1989).
38. H.-Y. Yuh and D. M. Pai, Mol. Cryst. Liq. Cryst. 183, 217 (1990).
39. P. M. Borsenberger, J. Appl. Phys. 68, 5188 (1990).
40. K. Nishimura, T. Kobata, H. Inada and Y. Shirota, J. Mater. Chem. 1, 897 (1991).
41. K. Nishimura, H. Inada, T. Kobata, Y. Matsui and Y. Shirota, Mol. Cryst. Liq. Cryst. 217, 235 (1992).
42. S. Nomura, K. Nishimura and Y. Shirota, Mol. Cryst. Liq. Cryst. 253, 79 (1994).
43. S. Nomura, K. Nishimura and Y. Shirota, Thin Solid Films 273, 27 (1996).
44. SAPI91: Fan Hai-Fu (1991). Structure Analysis Program with Intelligent Control, Rigaku Corporation, Tokyo, Japan.
45. P. T. Beurskens; DIRDIF: Direct methods for Difference Structures - an automatic procedure for phase extension and refinement of difference structure factors. Technical Report 1984/1 Crystallography Laboratory, Toernooiveld, 6525 Ed Nijmegen, Netherlands.
46. D. T. Cromer and J. T. Waber, International Tables for X-Ray Crystallography, Kynoch Press, Birmingham, England. Vol. IV, p. 71 (1974).
47. TEXSAN - TEXRAY Structure Analysis Package, Molecular Structure Corporation (1985).
48. W. C. Hamilton, Acta Cryst. 12, 609 (1959).
49. H. Scher and E. W. Montroll, Phys. Rev. B 12, 2445 (1975).
50. W. S. Sheldrick, W. Becker, and J. Engel, Acta Cryst. B34, 3120 (1978).
51. P. W. Codding, Acta Cryst. C43, 1394 (1987).

52. L. A. M. Baxter, A. J. Blake, R. O. Gould, G. A. Heath, and T. A. Stephenson, Acta Cryst. C49, 1311 (1993).
53. P. M. Borsenberger, J. Appl. Phys. 68, 6263 (1990).